

## **General Disclaimer**

### **One or more of the Following Statements may affect this Document**

- This document has been reproduced from the best copy furnished by the organizational source. It is being released in the interest of making available as much information as possible.
- This document may contain data, which exceeds the sheet parameters. It was furnished in this condition by the organizational source and is the best copy available.
- This document may contain tone-on-tone or color graphs, charts and/or pictures, which have been reproduced in black and white.
- This document is paginated as submitted by the original source.
- Portions of this document are not fully legible due to the historical nature of some of the material. However, it is the best reproduction available from the original submission.

# READ-WRITE HOLOGRAPHIC MEMORY WITH IRON-DOPED LITHIUM NIOBATE

BY

G. A. ALPHONSE AND W. PHILLIPS

(NASA-CR-143896) READ-WRITE HOLOGRAPHIC  
MEMORY WITH IRON-DOPED LITHIUM NIOBATE  
Final Report, 18 Oct. 1972 - 31 Mar. 1975  
(Radio Corp. of America) 39 p HC \$3.75

N75-27349

Unclass  
29217

CSCL 14E G3/35

## FINAL REPORT

MAY 1975

PREPARED UNDER CONTRACT NAS8-26808

RCA LABORATORIES  
PRINCETON, NEW JERSEY 08540

PREPARED FOR

GEORGE C. MARSHALL SPACE FLIGHT CENTER  
NATIONAL AERONAUTICS AND SPACE ADMINISTRATION  
HURTSVILLE, ALABAMA 35812



1. Report No.	2. Government Accession No.	3. Recipient's Catalog No.	
4. Title and Subtitle READ-WRITE HOLOGRAPHIC MEMORY WITH IRON-DOPED LITHIUM NIOBATE		5. Report Date May 1975	
		6. Performing Organization Code	
7. Author(s) G. A. Alphonse and W. Phillips		8. Performing Organization Report No. PRRL-75-CR-33	
9. Performing Organization Name and Address RCA Laboratories Princeton, New Jersey 08540		10. Work Unit No.	
		11. Contract or Grant No. NAS8-268C3	
12. Sponsoring Agency Name and Address George C. Marshall Space Flight Center National Aeronautics and Space Administration Huntsville, Alabama 35812		13. Type of Report and Period Covered Final Report	
		14. Sponsoring Agency Code	
15. Supplementary Notes			
16. Abstract The response of iron-doped lithium niobate under conditions corresponding to hologram storage and retrieval is described, and the material's characteristics are discussed. The optical sensitivity can be improved by heavy chemical reduction of lightly doped crystals such that most of the iron is in the divalent state, the remaining part being trivalent. The best reduction process found to be reproducible so far is the anneal of the doped crystal in the presence of a salt such as lithium carbonate. It is shown by analysis and simulation that a page-oriented read-write holographic memory with $10^3$ bits per page would have a cycle time of about 60 ms and a signal-to-noise ratio of 27 dB. This cycle time, although still too long for a practical system, represents an improvement of two orders of magnitude over that of previous laboratory prototypes using different storage media.			
17. Key Words (Selected by Author(s)) Holographic memory Read-write systems Hologram storage Lithium niobate		18. Distribution Statement	
19. Security Classif. (of this report) Unclassified	20. Security Classif. (of this page) Unclassified	21. No. of Pages 39	22. Price*

\*For sale by National Technical Information Service, Springfield, Virginia 22151.

## FOREWORD

This Final Report was prepared by RCA Laboratories, Princeton, New Jersey, for the NASA George C. Marshall Space Flight Center at Huntsville, Alabama. It describes work done under Contract NAS8-26808 during the period 18 October 1972 to 31 March 1975 in the Information Sciences Research Laboratory, Dr. Jan A. Rajchman, Staff Vice President and Director. The NASA Project Monitors were Mr. E. J. Reinbolt and Mr. G. A. Bailey.

Earlier efforts under this contract were reported in a comprehensive 3-volume interim report issued in November 1972 (refs. 1-3).

PRECEDING PAGE BLANK NOT FILMED

TABLE OF CONTENTS

Section	Page
SUMMARY . . . . .	1
I. INTRODUCTION . . . . .	2
II. MATERIAL CHARACTERIZATION . . . . .	4
A. Time Dependence of Holographic Storage and Erasure .	4
B. Optical Sensitivity . . . . .	9
C. Improving the Sensitivity of $\text{LiNbO}_3\text{:Fe}$ . . . . .	11
1. Sample Preparation by Argon Annealing . . . . .	i2
2. Sample Preparation by $\text{Li}_2\text{CO}_3$ Treatment . . . . .	13
3. Experiments with Reduction in Other Powdered Salts . . . . .	18
D. Spatial Frequency Response . . . . .	18
E. Noise Characteristics . . . . .	21
III. SYSTEMS CONSIDERATIONS . . . . .	24
A. Basic System . . . . .	24
B. Storage Medium Requirements . . . . .	25
1. High Resolution Capability . . . . .	25
2. Acceptable Dark Storage Time . . . . .	25
3. Acceptably Short and Equal Write and Erase Times . . . . .	25
4. Reversibility . . . . .	26
5. Low Noise . . . . .	26
C. Components Limitations and Projected Performance . .	26
D. Memory Simulation . . . . .	28
IV. CONCLUSIONS . . . . .	31
REFERENCES . . . . .	32

PRECEDING PAGE BLANK NOT FILMED

LIST OF ILLUSTRATIONS

Figure	Page
1. Setup for recording holograms in $\text{LiNbO}_3$ crystal . . . . .	6
2. Optical absorption of $\text{LiNbO}_3:\text{Fe}$ (0.005% Fe) annealed in argon and quenched (a) in water, (b) in air. The water-quenched crystal is fully reduced. The air-quenched crystal has about 65% of Fe as $\text{Fe}^{2+}$ . . . . .	14
3. Optical absorption of $\text{LiNbO}_3:\text{Fe}$ (0.002% Fe) annealed in $\text{Li}_2\text{CO}_3$ . Samples (a), (b), and (c) are annealed at $485^\circ\text{C}$ for 23 hours, 48 hours, and 82 hours, respectively. Sample (d) is annealed at $554^\circ\text{C}$ for 60 hours (fully reduced) . . . . .	15
4. Comparison of write-erase characteristics of different $\text{LiNbO}_3:\text{Fe}$ crystals. Dashed curve: heavily doped, lightly reduced; solid curve: lightly doped, heavily reduced in $\text{Li}_2\text{CO}_3$ . . . . .	17
5. Optical absorption of $\text{LiNbO}_3:\text{Fe}$ (0.002% Fe) annealed in salts other than $\text{Li}_2\text{CO}_3$ . (a) In $\text{Na}_2\text{CO}_3$ - annealed at $570^\circ\text{C}$ for 90 hours, (b) in $\text{Li}_2\text{SiO}_3$ - annealed at $570^\circ\text{C}$ for 80 hours, and (c) fully reduced $\text{Li}_2\text{CO}_3$ sample (as reference) . . . . .	19
6. Spatial frequency response of $\text{LiNbO}_3$ . In an optical memory, the "turning point" is the optimum location of the page composer . . . . .	20
7. Plot of the ratio of scattered light to incident light intensities as a function of exposure for a 0.1% Fe-doped $\text{LiNbO}_3$ crystal. After an exposure of about $1 \text{ J/cm}^2$ the induced noise builds up as the fourth power of the exposure . . . . .	21
8. Wiener noise spectrum of a typical $\text{LiNbO}_3:\text{Fe}$ crystal reduced in $\text{Li}_2\text{CO}_3$ . . . . .	23
9. Schematic of a read-write holographic memory from Ref. 23 . . . . .	24
10. Simulation of the light levels in a page-oriented read-write holographic memory with $10^3$ bits per page . . . . .	28
11. (a) Read-out signal of simulated memory (binary "1"). Horiz. = 20 ms/div., vert. = 2.5 nW/div. (b) Read-out of a "0" . . . . .	29

LIST OF TABLES

Table	Page
I. Summary of $\text{LiNbO}_3\text{:Fe}$ Preparation and Characteristics .	16
II. Comparison of the Wiener Noise of $\text{LiNbO}_3\text{:Fe}$ and of Other Storage Media at 1000 lines/mm . . . . .	23
III. Optical Memory Simulation Data . . . . .	30

READ-WRITE HOLOGRAPHIC MEMORY WITH  
IRON-DOPED LITHIUM NIOBATE

by

G. A. Alphonse and W. Phillips  
RCA Laboratories  
Princeton, New Jersey 08540

SUMMARY

The response of iron-doped lithium niobate under conditions corresponding to hologram storage and retrieval is described, and the material's characteristics are discussed. The optical sensitivity can be improved by heavy chemical reduction of lightly doped crystals such that most of the iron is in the divalent state, the remaining part being trivalent. The best reduction process found to be reproducible so far is the anneal of the doped crystal in the presence of a salt such as lithium carbonate. It is shown by analysis and simulation that a page-oriented read-write holographic memory with  $10^3$  bits per page would have a cycle time of about 60 ms and a signal-to-noise ratio of 27 dB. This cycle time, although still too long for a practical system, represents an improvement of two orders of magnitude over that of previous laboratory prototypes using different storage media.

## I. INTRODUCTION

The work at RCA and elsewhere on read-write holographic memory has shown that the component that poses the major problem in the realization of a system operating in the submillisecond cycle time is the storage medium. In an experimental memory built by RCA (ref. 4) the storage medium was thermoplastic. Although the sensitivity of thermoplastic is high, of the order of  $0.2 \mu\text{J}/\text{mm}^2$  for 1% diffraction efficiency, the memory cycle time is of the order of a few seconds, due to the required processing (charging and thermal fixing). A more suitable alternate storage medium is iron-doped lithium niobate. Its sensitivity has been improved considerably by means of a process that involved light doping of the material followed by heavy chemical reduction (ref. 5). The crystal is easy to grow and to handle, and the chemical treatment process seems to be reproducible.

In order to determine its usefulness as a potential storage medium, it is necessary to establish its characteristics. This includes the development of the preparation process that maximizes the sensitivity and the refinement of that process to achieve reproducibility. It also includes the theoretical and experimental study of the time development of the holographic storage and erasure, its dependence on beam modulation, recording angle, and its noise characteristics.

This Final Report deals with the progress that has been made in this effort and dwells on two major topics. The first is the material characterization per se. It includes the determination of the time response of the material to holographic stimulation, a discussion of the sensitivity and of the methods used at RCA to improve it, of the dependence of the holographic efficiency on recording angle, and of the noise characteristics. The second part discusses the systems requirements and limitations and uses the result of the time response analysis and the noise measurements to predict the performance of a read-write holographic

storage system using iron-doped  $\text{LiNbO}_3$ . The predicted performance is verified experimentally by means of measurements in a simulated read-write memory environment.

This work demonstrates that the sensitivity of lithium niobate doped with iron has been increased reproducibly by a factor of about 40, and that the noise characteristics have also been improved. It also indicates that a holographic read-write memory with a cycle time of about 60 ms and a high signal-to-noise ratio is now feasible with this material. Although this cycle time is still too low for a practical system, it does represent a two-order-of-magnitude improvement over earlier prototypes (ref. 4).

## II. MATERIAL CHARACTERIZATION

### A. Time Dependence of Holographic Storage and Erasure

In an effort to characterize the iron-doped lithium niobate ( $\text{LiNbO}_3:\text{Fe}$ ) samples, some of the most important questions that must be answered are: For a given holographic illumination, how much time does it take for the diffraction efficiency to reach a certain value? How does that time depend on the illumination level? What is the time constant for erasure? What determines the material's optical sensitivity? What parameters must be manipulated chemically in material preparation to improve that sensitivity? The answer to those questions lies in the rigorous analysis of the complete space-time development of holograms under writing and erasing illuminations.

When exposed to light, a number of electrooptic ferroelectric or photorefractive materials exhibit refractive index changes (ref. 6). These changes are attributed to electrooptic effects due to the storage of electric fields (ref. 7) in the material as a result of the optical exposure. For very intense light (of the order of several  $\text{W}/\text{mm}^2$ ) the stored electric field is the result of macroscopic polarization changes in the material due to nonlinear absorption (ref. 8). For light of moderate intensities (less than a few hundred  $\text{mW}/\text{mm}^2$ ) the mechanism of electric field storage is that of space-charge migration (refs. 7,9). It is this space-charge model that applies to holographic storage in read-write memory systems of the type under study in this work. In this model electrons are excited from impurity traps by the incident radiation and, upon migration, are retrapped at other locations, giving rise to a frozen-in electric field. The latter induces refractive index changes via the electrooptic effect. In undoped crystals the traps are provided by small traces of impurities. In doped crystals, the dopants act as donor-acceptor traps via intervalence exchanges such as  $\text{Fe}^{2+} \rightleftharpoons \text{Fe}^{3+}$  in  $\text{LiNbO}_3:\text{Fe}$  (ref. 5,10). In general, the migration of

charges occurs under the combined influence of diffusion and an electric field. The electric field may be internally generated or externally applied. Although the space-charge field can have arbitrary directions, only the component along the optic or c-axis is of most interest to holographers because of the relative size of the  $r_{33}$  electrooptic coefficient compared with the other coefficients (ref. 11). This field causes a change to occur mainly in the extraordinary refractive index without affecting the other optical properties of the material. This refractive index change  $\Delta n_e$  is given by (ref. 12)

$$\Delta n_e = -\frac{1}{2} n_e^3 r_{33} E_s, \quad (1)$$

where  $n_e$  is the extraordinary refractive index,  $r_{33}$  is the third diagonal component of the electrooptic tensor, and  $E_s$  the stored electric field along the optic axis. When the illumination is spatially periodic,  $E_s$  is also periodic and the refractive index pattern is the hologram.

The stored electric field under spatially periodic illumination, as in hologram formation, has been calculated from the space charge model (ref. 13). The results from ref. 13 that apply to the subject of this report are summarized below. When the medium, oriented as shown in Fig. 1, is illuminated by beams  $I_1$  (object) and  $I_2$  (reference) at the incidence angles  $\pm \theta$ , respectively, the total illumination  $I$ , as a function of the z-coordinate, is given by

$$I(z) = I_0 (1 + m \cos Kz), \quad (2)$$

where  $I_0$  is the sum of the intensities  $I_1$  and  $I_2$ ,  $m = 2\sqrt{I_1 I_2}/I_0$  is the modulation index, and  $K$  is the angular frequency, given by

$$K = \frac{4\pi}{\lambda} \sin \theta, \quad (3)$$

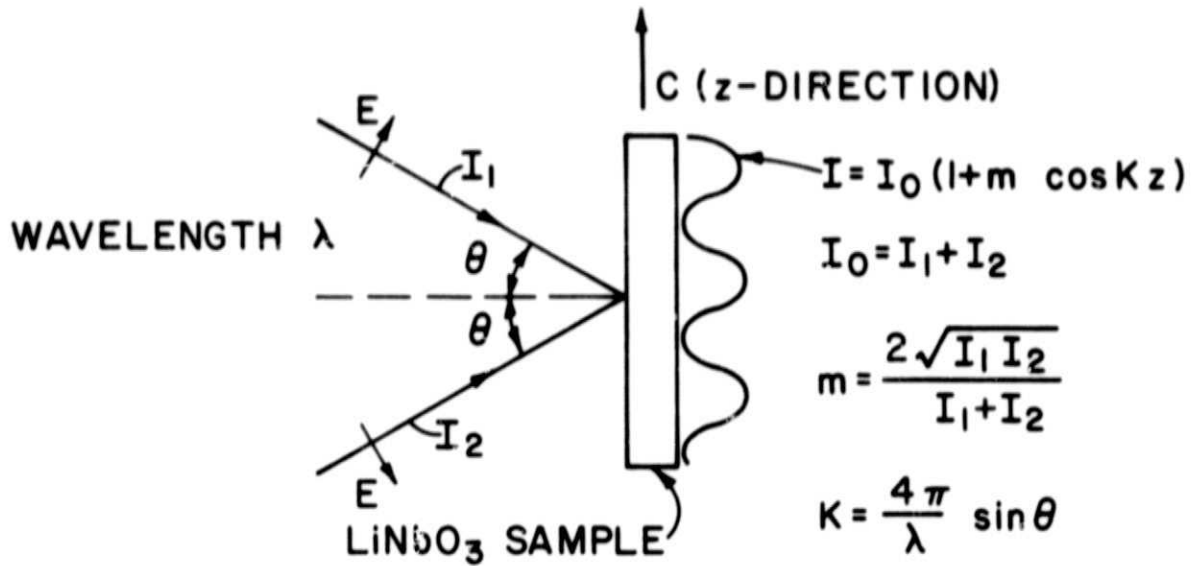


Figure 1. Setup for recording holograms in LiNbO<sub>3</sub> crystal.

where  $\lambda$  is the wavelength of the incident light. It is assumed that the lifetime  $\tau$  of the photoexcited electrons is much shorter (of the order of  $10^{-11}$  s) than the dielectric relaxation time. The lifetime is given by (refs. 14,15)

$$\tau = \frac{1}{N_e V S}, \quad (4)$$

where  $N_e$  is the density of empty (or acceptor) traps in the material,  $V$  the thermal velocity of the electrons, and  $S$  their capture cross section. The dielectric relaxation time  $T_0$  is given by

$$T_0 = \frac{\epsilon}{n_0 q \mu}, \quad (5)$$

where  $\epsilon$  is the dielectric constant,  $n_0$  the average concentration of the photoexcited electrons,  $q$  the electronic charge, and  $\mu$  the mobility. It

is also assumed that the migration length  $L$ . (Average distance travelled during a lifetime is such that  $KL \ll 1$ ; from ref. 13 this is true for  $\theta$  less than about  $23^\circ$ .) Under those conditions the electron concentration  $n$  is just the product of the lifetime and the generation rate  $g$ , i.e.,

$$n = \tau g, \quad (6)$$

where (ref. 9)

$$g = \frac{\sigma N_f}{h\nu} I(z), \quad (7)$$

and where  $\sigma$  is the absorption cross section,  $N_f$  is the density of filled (or donor) traps,  $h$  is Planck's constant, and  $\nu$  is the optical frequency. It is convenient to write Eqs. (6) and (7) as

$$n = n_o (1 + m \cos Kz) = n_o n(z),$$

where

$$n_o = \frac{\sigma N_f}{h\nu} \tau I_o \quad (9)$$

is the average concentration discussed earlier, and where

$$n(z) = 1 + m \cos Kz. \quad (10)$$

The current density is

$$\underline{J} = qDn_o \nabla n(z) + q n_o n(z) \underline{E}, \quad (11)$$

where  $D$  is the electrons' diffusion constant, and  $\underline{E}$  is the total electric field, equal to the sum of the stored field  $\underline{E}_s$  and of any dc field

$E_a$  that may be applied or that may exist within the material. In ref. 13 it is shown that when all this information is substituted into the continuity equation

$$\nabla \cdot \underline{J} + \epsilon \left( \frac{\partial E}{\partial t} \right) = 0, \quad (12)$$

the magnitude of stored electric field (in the z-direction) is

$$E_s(z,t) = \frac{m}{n(z)} E_{\max} \left\{ 1 - \exp[-n(z)t/T_0] \right\} \sin(Kz - \phi), \quad (13)$$

where

$$E_{\max} = \left[ \left( K \frac{kT}{q} \right)^2 + E_a^2 \right]^{1/2} \quad (14)$$

$$\phi = \tan^{-1} \left( \frac{qE_a}{K k T} \right), \quad (15)$$

and where  $k$  is Boltzman's constant,  $T$  is the absolute temperature, and  $E_a$  is assumed to be along the z-axis. Due to the factor  $n(z)$  in the denominator and in the exponential,  $E_s$  contains several harmonics. However, when the object consists of a large number of light spots at discrete locations, the light from each spot or bit creates an illumination in the form of Eq. (2), with  $m \ll 1$ , and Eq. (13) reduces to the simple sinusoid

$$E_s(z,t) = m E_{\max} [1 - \exp(-t/T_0)] \sin(Kz - \phi). \quad (16)$$

This field can be permanently "fixed" in the material (ref. 16). If no fixing is done, then upon constant illumination the stored electric field is erased. If the initial value is  $E_0(z)$ , the field decays

$$E_s(z,t) = E_0(z) \exp(-t/T_0). \quad (17)$$

As mentioned earlier, the stored field gives rise to a refractive index change [Eq. (1)] which constitutes a phase hologram or grating. The hologram of an arbitrary object or of a distribution of point sources is a superposition of the individual gratings made by the interference of the reference beam and the point sources constituting the object.

For read-out, the hologram is exposed to the reference beam alone, polarized extraordinarily, in order that its propagation be affected by  $\Delta n_e$ . Since the hologram's thickness is of the order of 1 mm, equivalent to about 2000 optical wavelengths, and since the reference beam is at the Bragg angle, the diffracted light is a reconstruction of the object beam. The diffraction efficiency  $\eta$ , for negligible absorption, is given by (ref. 17)

$$\eta = \sin^2 \left( \frac{\pi \ell |\Delta n_e|}{\lambda \cos \theta} \right), \quad (18)$$

where  $\ell$  is the hologram's thickness. In practice the absorption constant  $\alpha$  is nonnegligible, and if it is considered uniform, the efficiency is reduced by a factor of  $\exp(-2 \alpha \ell)$ . Moreover, the quantity in parentheses in Eq. (18) is often much less than  $\pi/2$ . This gives

$$\eta \approx \left[ \frac{\pi \ell |\Delta n|}{\lambda \cos \theta} \right]^2 \exp(-2 \alpha \ell). \quad (19)$$

The effect of the absorption can severely limit the efficiency. For example, if  $\alpha$  is large, differentiation of Eq. (19) with respect to  $\ell$  shows that the optimum thickness is  $\ell = 1/\alpha$  and that the maximum efficiency is 14%. It must be noted that if the hologram is not fixed, reading it out will also erase it, a desirable feature for short cycle time in read-write applications.

### B. Optical Sensitivity

It follows from Eq. (16) that for  $m \ll 1$  the relaxation time  $T_0$ , which is the time constant for the decay [Eq. (17)] of the stored field

of the hologram, is also the time constant for its build-up. It is inversely proportional to the illumination. By combining Eqs. (4), (5), and (9) we find

$$T_0 = C/I_0, \quad (20)$$

where

$$C = \frac{\epsilon h \nu V S}{q \mu \sigma} \frac{N_e}{N_f}, \quad (21)$$

and where  $N_e/N_f$  is the ratio of the empty traps to the filled traps. In  $\text{LiNbO}_3:\text{Fe}$  this ratio is that of the  $\text{Fe}^{3+}$  to the  $\text{Fe}^{2+}$  concentrations. We note that for a given sample,  $C$  is a constant that is proportional to the ratio of empty-to-filled trap concentrations. The smaller  $C$ , the smaller  $T_0$  for a given illumination and the faster the build-up or erasure of a hologram. It is thus appropriate to designate  $C$  as the parameter that represents the sensitivity of a sample. Its units are that of energy density (if  $I_0$  is in  $\text{mW/mm}^2$ , then  $C$  is in  $\text{mJ/mm}^2$ ), and it can be obtained experimentally by measuring the decay time constant of a hologram using a known uniform illumination. Indeed, the stored field decays as  $\epsilon^{-t/T_0}$  or  $\epsilon^{-I_0 t/C}$ , and the holographic efficiency  $\eta$  decays from an initial value  $\eta_0$  as the square of the field, i.e.,

$$\eta/\eta_0 = \epsilon^{-2I_0 t/C} \quad (22)$$

A comparison of the value of  $C$  for different samples is in fact a comparison of their respective sensitivities. This is the procedure that has been used, together with the measurement of the peak efficiency and the dark storage time constant, to evaluate the suitability of the iron-doped lithium niobate samples prepared under this contract for read-write applications. This parameter  $C$  has also been used to obtain expressions for the write and erase times (cycle time) of holographic memories.

### C. Improving the Sensitivity of $\text{LiNbO}_3:\text{Fe}$

The most important aim of the work to improve the sensitivity of our samples involves two points: Developing procedures in material preparation that will minimize C and developing techniques that will make the procedure reproducible. The highest sensitivity is obtained when the crystal has a low overall iron concentration and is treated so that all but about 10% of the iron is reduced to the divalent ( $\text{Fe}^{2+}$ ) state, the rest of the iron remaining trivalent ( $\text{Fe}^{3+}$ ). That this criterion is correct can be verified from the expression for the sensitivity parameter C [Eq. (21)], and from the expression for the diffraction efficiency [Eq. (19)] in the presence of absorption. Indeed, because C is proportional to the ratio of  $\text{Fe}^{3+}$  to  $\text{Fe}^{2+}$  concentrations, the smaller the ratio, the smaller C, i.e., the higher the sensitivity. However, since the absorption of the material is determined by the  $\text{Fe}^{2+}$  concentration, excessive absorption would seriously reduce the diffraction efficiency; hence, the need for the overall absorption to be low.

Two procedures have been employed to reduce the  $\text{Fe}^{3+}$  concentration to low levels. In the first, crystals are annealed in argon at a temperature near  $1100^\circ\text{C}$ , then are cooled rapidly to room temperature. In the second, they are annealed at  $550$  to  $600^\circ\text{C}$  while packed in powdered  $\text{Li}_2\text{CO}_3$  in an air or oxygen ambient. In addition to providing crystals to use in the holographic memory research program, the materials study portion of this contract has been aimed at determining whether either of those methods could be developed to produce low  $\text{Fe}^{3+}$  concentration crystals with predictable characteristics on a reproducible basis. The problem anticipated for each approach can be summarized briefly as follows.

When iron-doped crystals are annealed in argon, the  $\text{Fe}^{2+}$  concentration reaches a high value. However, the  $\text{Fe}^{2+}$  reoxidizes as the temperature is lowered, making it difficult to retain more than roughly 50% of the iron in the divalent state. If the crystals are cooled rapidly from the anneal temperature, more  $\text{Fe}^{2+}$  is retained, and this

"quenched-in" concentration is stable at room temperature. The amount of  $\text{Fe}^{2+}$  retained depends on the cooling rate, which in turn depends on the size of the crystal, its placement in the furnace tube, and other variables that are difficult to control.

On the other hand, annealing of iron-doped crystals in powdered  $\text{Li}_2\text{CO}_3$  produces reduction of the iron by virtue of lithium ions diffusing into the crystal. This occurs at a comparatively low temperature (500 to 600°C), and the  $\text{Fe}^{2+}$  concentration thus produced is dependent of the cooling rate. However, relatively little is understood about this process and two questions in particular had to be investigated: First, are crystals produced in this manner equivalent to those produced in argon in terms of storage characteristics? Second, how does the  $\text{Fe}^{2+}$  concentration thus produced depend on the temperature and time of anneal? In addition, a third problem arises due to increased thermal erasure of  $\text{Li}_2\text{CO}_3$ -reduced crystals. The work to be described was performed on slices of a  $\text{LiNbO}_3$  crystal doped with 0.002% Fe purchased from Crystal Technology, Inc. The slices were oriented to lie in the x-z plane. The doping was chosen so that heavily reduced crystals of a convenient thickness ( $\sim 2.1$  mm) would absorb 1/2 to 3/4 of the incident light at 4880 Å.

1. Sample Preparation by Argon Annealing. - It is estimated that the cooling rate necessary to "quench-in" about 90% of the  $\text{Fe}^{2+}$  population in argon-reduced crystals would be on the order of 10°C per second, limited by heat loss of the samples and of their support structure. Two experiments were performed to define the degree of difficulty to be encountered in this approach. In both cases, crystals were placed in a 1.25-in. ID quartz tube furnace and annealed at 1100°C for 16 hours. In the first case, samples were placed in a platinum foil-lined alumina boat. At the end of the anneal, the entire quartz tube assembly was pushed out of the furnace and allowed to cool in the air. In the second experiment, a crystal was supported only by platinum foil. When the

quartz tube was pushed out of the furnace after the anneal, it was cooled very rapidly with water.

The optical absorption of the two crystals is shown in Fig. 2. The air-quenched crystal has only about 65% of the absorption of the water-quenched crystal. The diffraction efficiency of holograms written in the water-quenched crystal is extremely small, of the order of  $10^{-2}\%$ . This indicates that there is essentially no  $\text{Fe}^{3+}$  in the crystal. The optical absorption of the air-quenched crystal, on the other hand, indicates that only 65% of the Fe is divalent, the rest presumed to be trivalent. Since this relative concentration of  $\text{Fe}^{3+}$  to  $\text{Fe}^{2+}$  is not optimum, it would be necessary to build an apparatus that would give a cooling rate between that of the water-quenching and the air-quenching. This approach was not pursued, however, in view of the excellent results obtained by the  $\text{Li}_2\text{CO}_3$  annealing process described below.

2. Sample Preparation by  $\text{Li}_2\text{CO}_3$  Treatment. - The procedure for  $\text{Li}_2\text{CO}_3$  sample preparation is to bury one or more unpolished crystals in powdered  $\text{Li}_2\text{CO}_3$  contained in a small platinum crucible. The crucible is then heated in an oxygen atmosphere. The temperature is monitored independently of the control thermocouple by means of a second thermocouple placed at the top of the crucible. At the end of the anneal the  $\text{Li}_2\text{CO}_3$  powder is discarded and the crystals are polished.

It is generally known that heavy coloration of the crystals would take place in the 500 to 550°C temperature range. However, insufficient information was available as to whether the reduction of crystals treated at the low end of this temperature range would reach equilibrium at some predetermined level below 100%, reduction influenced only by the temperature. To provide an answer to this question, crystals were annealed in  $\text{Li}_2\text{CO}_3$  for varying times and temperatures. A sample annealed at 554°C for 60 hours was found to have absorption quite comparable to the water-quenched argon-annealed sample described earlier. This sample is assumed to be close to 100% reduced. However, other samples prepared

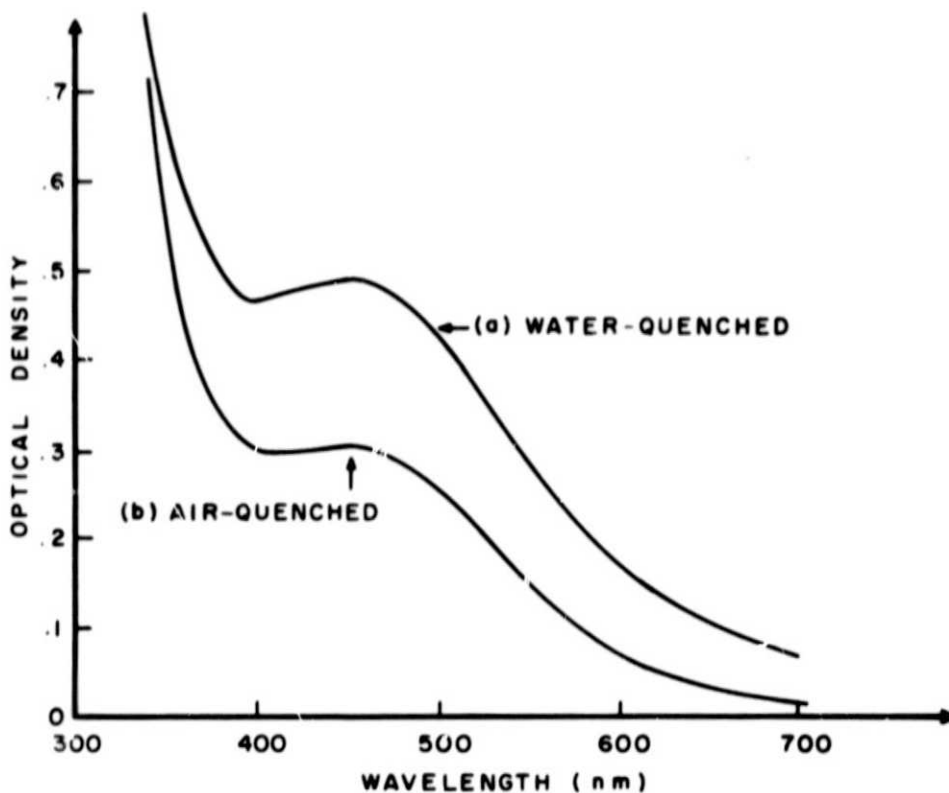


Figure 2. Optical absorption of LiNbO<sub>3</sub>:Fe (0.005% Fe) annealed in argon and quenched (a) in water, (b) in air. The water-quenched crystal is fully reduced. The air-quenched crystal has about 65% of Fe as Fe<sup>2+</sup>.

at lower temperatures (486° to 500°C) have less absorption (corresponding to 85 to 90% reduction) even after extended anneal times. This indicates that the Li<sub>2</sub>CO<sub>3</sub> process can be used to control the Fe<sup>2+</sup> to Fe<sup>3+</sup> ratio in the 85 to 95% region on an equilibrium basis; this is an important point that signifies that the process is amenable to close control and high reproducibility. The absorption data for a representative selection of crystals are shown in Fig. 3.

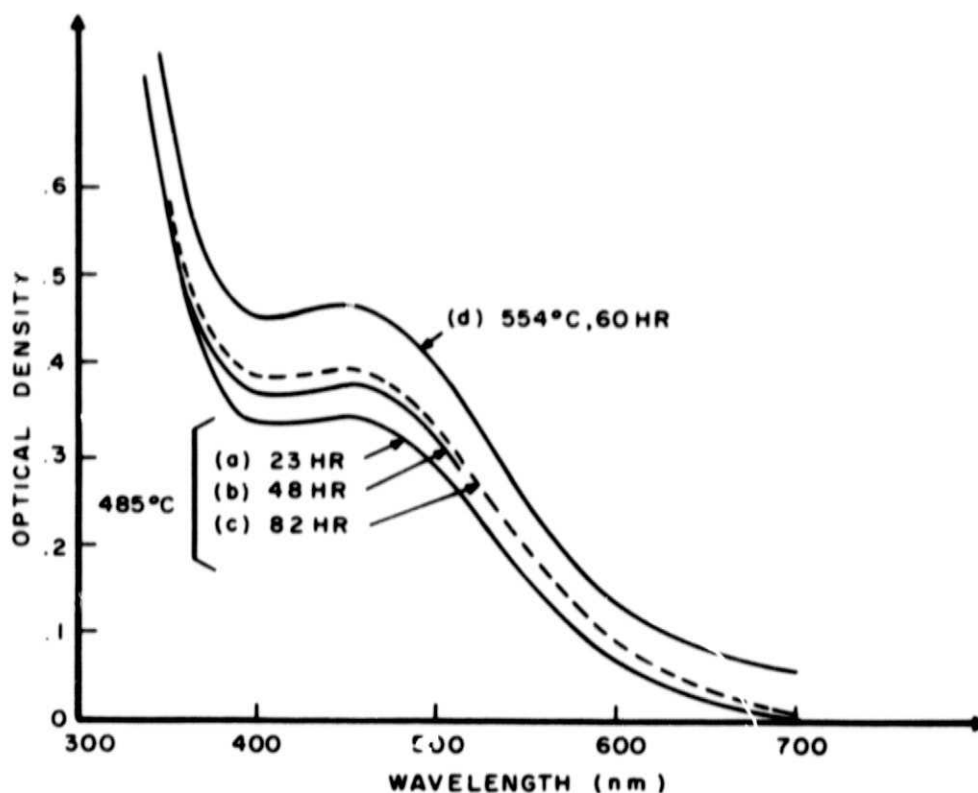


Figure 3. Optical absorption of  $\text{LiNbO}_3:\text{Fe}$  (0.002%) annealed in  $\text{Li}_2\text{CO}_3$ . Samples (a), (b), and (c) are annealed at  $485^\circ\text{C}$  for 23 hours, 48 hours, and 82 hours, respectively. Sample (d) is annealed at  $554^\circ\text{C}$  for 60 hours (fully reduced).

Table I is a summary of the characteristics of several samples prepared according to the two procedures. The argon-annealed water-quenched sample and the  $554^\circ\text{C}$   $\text{Li}_2\text{CO}_3$  samples, which are presumed to be fully reduced (100%  $\text{Fe}^{2+}$ ) did not store holograms with measurable diffraction efficiency. The air-quenched argon-reduced sample shows good sensitivity with  $C = 2.2 \text{ mJ/mm}^2$  and extremely long dark storage time constant (100 days). By comparison, a typical sample with 1% iron and 15% reduced, made prior to the development of either reduction technique, had  $C = 65 \text{ mJ/mm}^2$ . The most sensitive sample is the 48-hour,

Table I. - Summary of  $\text{LiNbO}_3:\text{Fe}$  Preparation and Characteristics.\*

Preparation*			Percent $\text{Fe}^{2+}$	Optical Density at 450 nm	$C^{**}$ $\text{mJ/mm}^2$	Dark Storage Time Constant
Anneal Temp.	Time (hr)	Method				
1100°C-Ar	60	Water quench	100	0.48	-	-
1100°C-Ar	23	Air quench	65	0.3	2.2	100 days
554°C	60	$\text{Li}_2\text{CO}_3$	100	0.44	-	-
485°C	82	"	88	0.39	2.64	>100 hr
485°C	23	"	77	0.34	2.1	>400 hr
485°C	48	"	86	0.38	1.75	>100 hr
500°C	90	"	90	0.40	-	-

\*Argon anneal samples, 0.005% Fe;  $\text{Li}_2\text{CO}_3$  annealed samples, 0.002% Fe.  
\*\*By comparison, a sample with 0.1% iron having 15% of  $\text{Fe}^{2+}$  has  
 $C = 65 \text{ mJ/mm}^2$ .

485°C  $\text{Li}_2\text{CO}_3$ -reduced sample. It has a sensitivity of  $1.76 \text{ mJ/mm}^2$ , an improvement by a factor of 38 over the earlier 0.1% Fe sample. The  $\text{Li}_2\text{CO}_3$ -reduced samples have a shorter dark storage time constant than the argon-reduced samples. The explanation of this is not known at the present time. We also do not know the explanation for the fact that the 500°C sample annealed for 90 hours would not store holograms, in spite of the fact that it does not appear to be 100% reduced. One can postulate however, that the conductivity of the samples continues to build up during  $\text{Li}_2\text{CO}_3$  reduction even after the  $\text{Fe}^{2+}$  concentration has reached equilibrium. Thus, the crystal annealed for 90 hours had too much conductivity for a significant field to build up during hologram formation.

Figure 4 shows a comparison of the write-erase characteristics of holograms made in the 0.1% Fe-doped lightly reduced (15%) crystal and

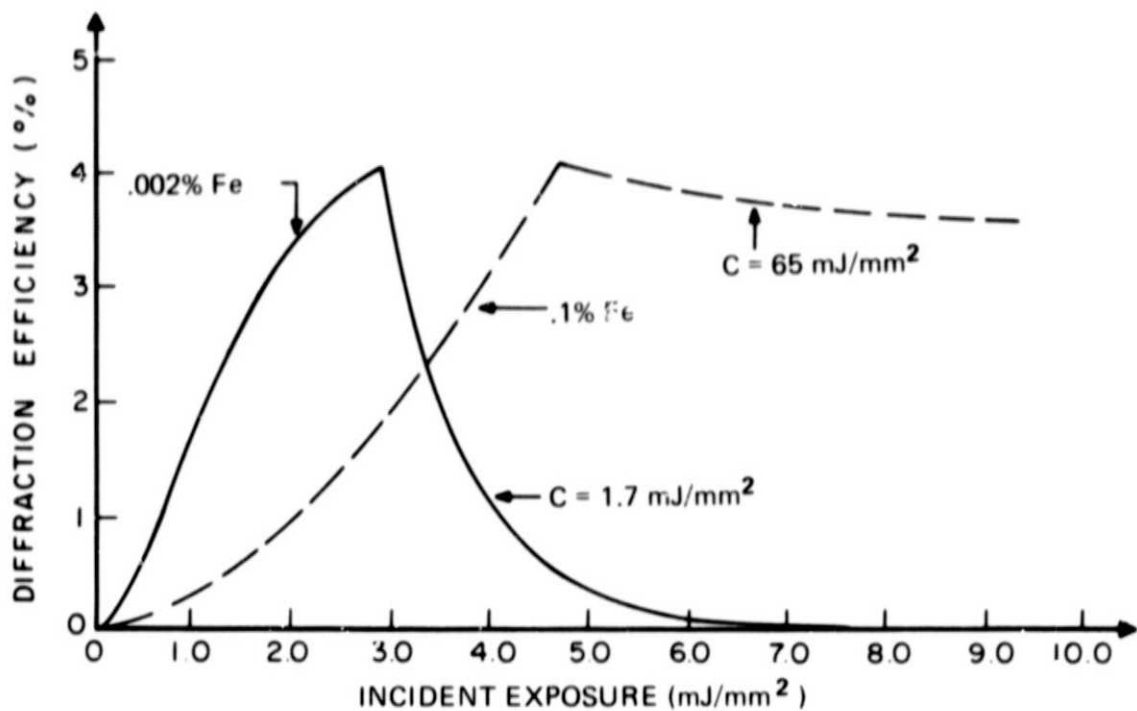


Figure 4. Comparison of write-erase characteristics of different  $\text{LiNbO}_3:\text{Fe}$  crystals. Dashed curve: heavily doped, lightly reduced; solid curve: lightly doped, heavily reduced in  $\text{Li}_2\text{CO}_3$ .

in one of the  $\text{Li}_2\text{CO}_3$ -reduced samples. The 0.1% Fe-doped sample, which has a value of  $C = 65 \text{ mJ/mm}^2$ , is slow to erase but is capable of high diffraction efficiency (dashed curve). On the other hand, the 0.002% doped crystal (solid curve), which is 86% reduced with  $C = 1.7 \text{ mJ/mm}^2$ , has a much lower saturation efficiency but requires less than  $2 \text{ mJ/mm}^2$  to erase significantly. The low efficiency is due to the absorption of the  $\text{Fe}^{2+}$ . It was also found that the optically induced scattering noise present in the 0.1% doped crystal does not exist in the lightly doped crystal reduced by either process. This fact has been observed in all the samples that exhibit low diffraction efficiency.

3. Experiments with Reduction in Other Powdered Salts. - We also explored the possibility of using powdered salts other than  $\text{Li}_2\text{O}$  to perform the heavy but incomplete reductions required. Two salts in particular were tried,  $\text{Li}_2\text{SiO}_3$  and  $\text{Na}_2\text{CO}_3$ . The latter was of particular interest because reduction via sodium ions might be expected to produce somewhat different properties than lithium reduction, and perhaps lead to longer dark storage times. The absorption curves produced by the longest anneals in each of these salts are shown in Fig. 5. For comparison we also show a 100% argon-reduced crystal. Although reduction in these salts yields the expected  $\text{Fe}^{2+}$  absorption spectrum, the fractional conversion to  $\text{Fe}^{2+}$  is relatively small. The hologram storage sensitivity of these crystals was very low, as would be expected for crystals with large  $\text{Fe}^{3+}$  concentrations.

Although the optical absorption produced by annealing in  $\text{Li}_2\text{SiO}_3$  and  $\text{Na}_2\text{CO}_3$  was continuing to increase, the time that would have been required to approach 90% reduction was prohibitively long and so this line of investigation was stopped.

#### D. Spatial Frequency Response

The spatial frequency response is a plot of the holographic efficiency vs recording angle expressed in spatial frequency, at constant recording energy and modulation index. This response determines the allowable range of spatial frequencies for the page composer and the uniformity of the output signal. In the absence of the applied field  $E_a$  (a practical consideration in the design of a system), Eqs. (13) and (14) predict that the stored field is proportional to  $K$  which, according to Eq. (3), is proportional to the sine of half the recording angle, i.e.,  $K = (4\pi/\lambda) \sin \theta$ . The efficiency, according to our theory, is thus proportional to  $K^2$ . However, the theory is valid only as long as the electron pattern remains a replica of the illumination, without smearing out. If  $L = (D\tau)^{1/2} = (kT \mu\tau/q)^{1/2}$  is the diffusion length of the electrons in the material, the  $K^2$  dependence will be true as long

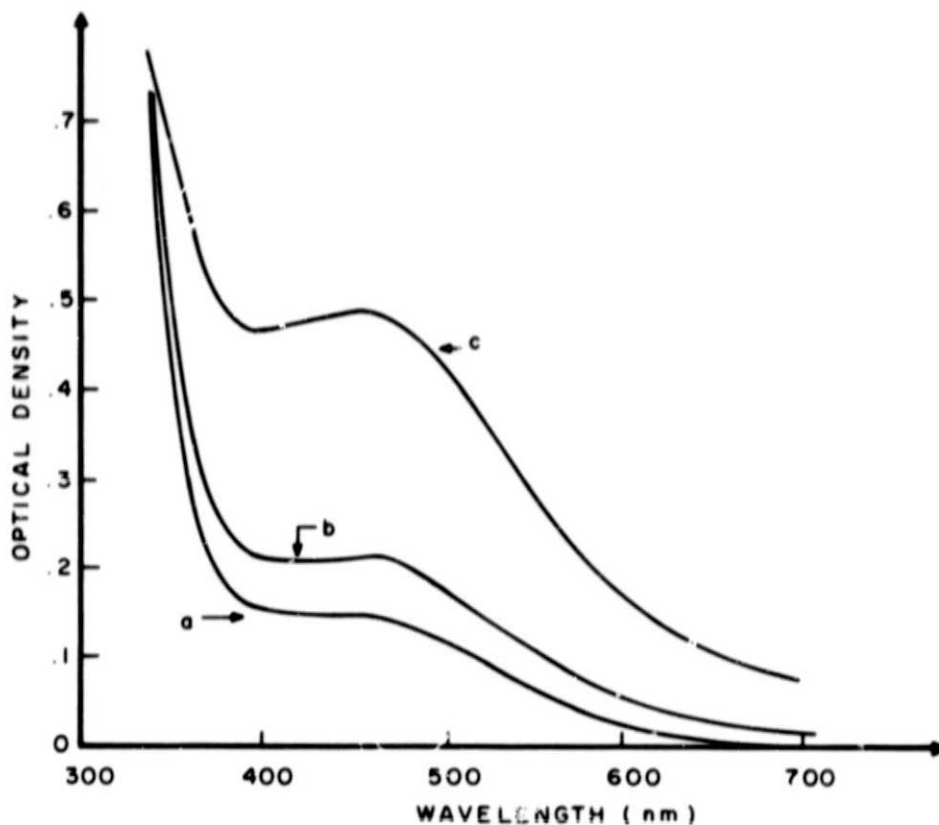


Figure 5. Optical absorption of  $\text{LiNbO}_3:\text{Fe}$  (0.002% Fe) annealed in salts other than  $\text{Li}_2\text{CO}_3$ . (a) In  $\text{Na}_2\text{CO}_3$  - annealed at  $570^\circ\text{C}$  for 90 hours, (b) in  $\text{Li}_2\text{SiO}_3$  - annealed at  $570^\circ\text{C}$  for 80 hours, and (c) fully reduced  $\text{Li}_2\text{CO}_3$  sample (as reference).

as  $KL \ll 1$ . For larger values of  $K$  the holographic efficiency will fall off as a result of the smearing of the electron pattern. The spatial frequency response is shown in Fig. 6 as a plot of holographic efficiency vs the spatial frequency  $f = K/2\pi$  lines/mm. For each data point the recording is  $2.3 \text{ mJ/mm}^3$ , and the modulation index is unity. The value of  $C$  for the sample is  $2.2 \text{ mJ/mm}^2$  and the thickness is 1.7 mm. The expected  $K^2$  dependence is shown to exist up to a spatial frequency of  $f \cong 1600$  lines/mm, corresponding to  $\theta \cong 23^\circ$  or  $K = 10^4$  per mm,

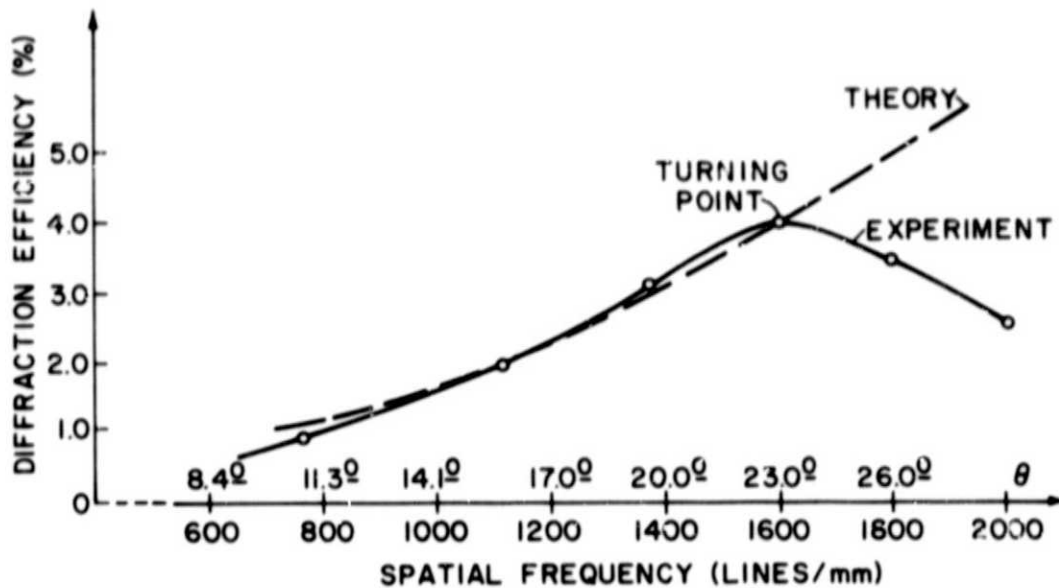


Figure 6. Spatial frequency response of  $\text{LiNbO}_3$ . In an optical memory, the "turning point" is the optimum location of the page composer.

followed by a roll-off approximately as  $(1/K)^2$ . A calculation (ref. 18) using  $\mu \cong 16 \text{ cm}^2/\text{V-s}$  and  $\tau \cong 4 \times 10^{-11} \text{ s}$  gives  $L \cong 4 \times 10^{-5} \text{ mm}$  and  $KL = 0.4$  at the "turning point". The roll-off above the turning point is consistent with a theory by Young and co-workers (ref. 18) for the initial time development, in which the restriction on the migration length is removed.

From a systems viewpoint the "turning point" indicates the optimum spatial carrier frequency or location of the page composer, for only around that point is the storage medium's response essentially flat over some spatial frequency bandwidth. For the sample under discussion, the half-power response is from 1350 lines/mm to about 1900 lines/mm centered at 1600 lines/mm.

### E. Noise Characteristics

In the read-out of an optical system, any undesired light falling upon the photodetector array tends to reduce the image contrast and can be considered as noise. In lithium niobate, in addition to the usual noise due to scattering from imperfections in the crystal, there is often an optically induced scattering (refs. 19, 20) that builds up negligibly initially as a function of exposure, then rises rapidly as a fourth power law of the exposure. This behavior is illustrated in Fig. 7. In the so-called "static" region the noise contribution is

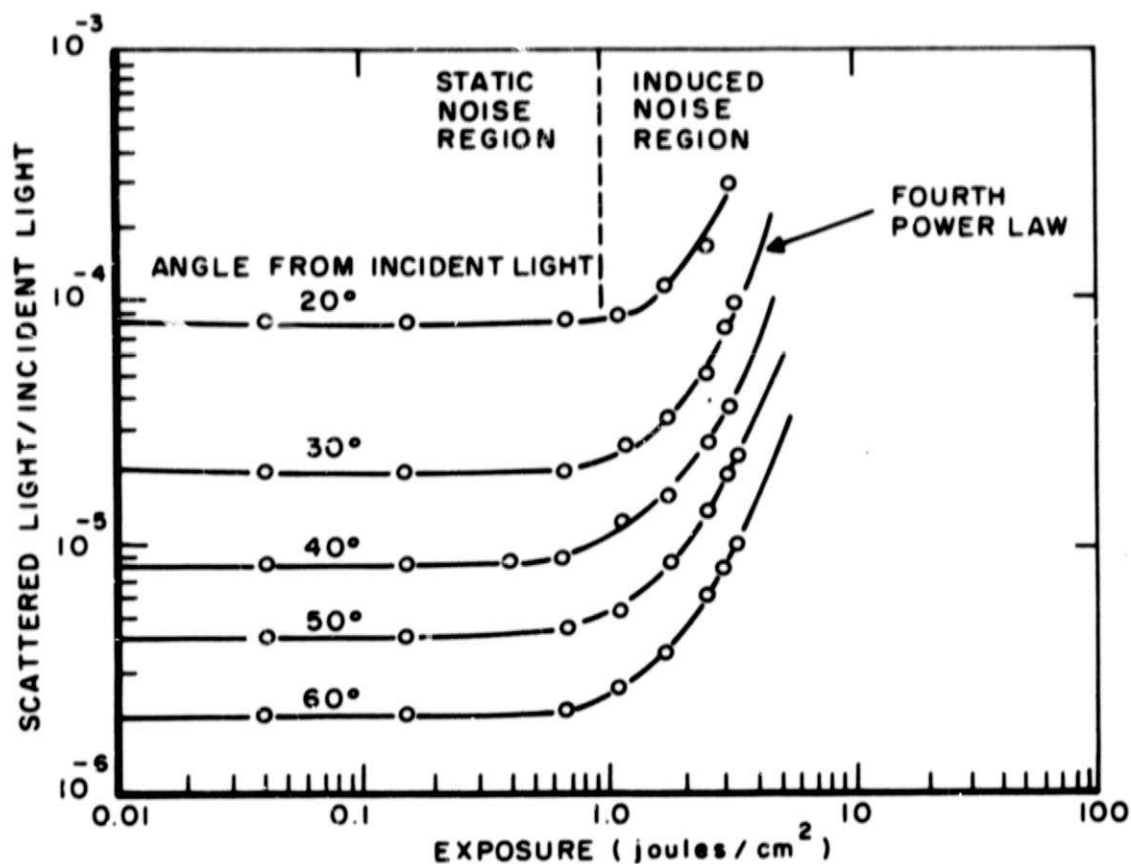


Figure 7. Plot of the ratio of scattered light to incident light intensities as a function of exposure for a 0.1% Fe-doped LiNbO<sub>3</sub> crystal. After an exposure of about 1 J/cm<sup>2</sup> the induced noise builds up as the fourth power of the exposure.

mainly from the usual scattering process. The induced noise appears only at high exposure. It is accompanied by distortion in the transmitted beam and exhibits the same properties as the holograms made in the sample: growth with exposure, angular sensitivity, polarization dependence, etc. The experimental evidence indicates that it is the result first of a gradual bending of part of the reference beam followed by the interference between the bent and unbent portions of the reference beam. The ray bending is due to optically induced local index inhomogeneities due to the possibly nonuniform cross section of the beam. The interference pattern is then recorded as a hologram. Experimentally, this scattering is found to occur only in samples capable of high diffraction efficiency. This optically induced noise does not seem to appear in the materials having improved sensitivity. It must be noted that the saturation efficiency of those materials is usually low, of the order to a few percent, possibly due to the effect of absorption. Thus, for all practical purposes, only the static noise is present in those samples.

The Wiener noise spectrum for a typical  $\text{Li}_2\text{CO}_3$ -reduced sample is shown in Fig. 8. A comparison of the Wiener noise at 1000 lines/mm for several materials (ref. 21), including  $\text{Li}_2\text{CO}_3$ -reduced iron-doped lithium niobate, is shown in Table II. It is seen that  $\text{LiNbO}_3$  compares well with dichromated gelatin (DCG) (used as a reference) and may have a slightly better noise characteristic.

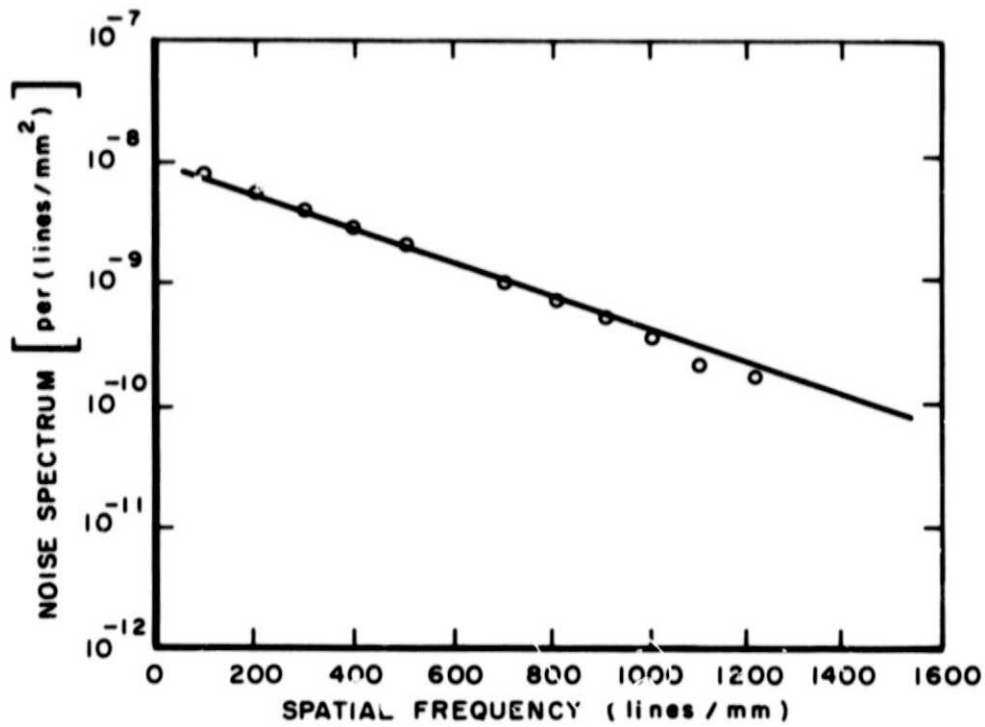


Figure 8. Wiener noise spectrum of a typical LiNbO<sub>3</sub>:Fe crystal reduced in Li<sub>2</sub>CO<sub>3</sub>.

Table II. - Comparison of the Wiener Noise of LiNbO<sub>3</sub>:Fe and of Other Storage Media at 1000 lines/mm.

<u>Material</u>	<u>Wiener Noise at 1000 lines/mm</u>	<u>Relative with Respect to DCG</u>
DCG (Dichromated gelatin)	8 x 10 <sup>-10</sup>	1.0
Kodak 649F at 50% Transmission	8 x 10 <sup>-8</sup>	100
Afga 10E70 at 50% Transmission	2.5 x 10 <sup>-8</sup>	31
Bleached Kodak 649F	9 x 10 <sup>-8</sup>	112
Li <sub>2</sub> CO <sub>3</sub> - Reduced LiNbO <sub>3</sub> :Fe	5 x 10 <sup>-10</sup>	0.625

### III. SYSTEMS CONSIDERATIONS

#### A. Basic System

The basic configuration of a holographic memory (ref. 5) is shown in Fig. 9. It consists of a laser source, a deflection system, a hololens, a page composer, the storage medium, and a detector array. The

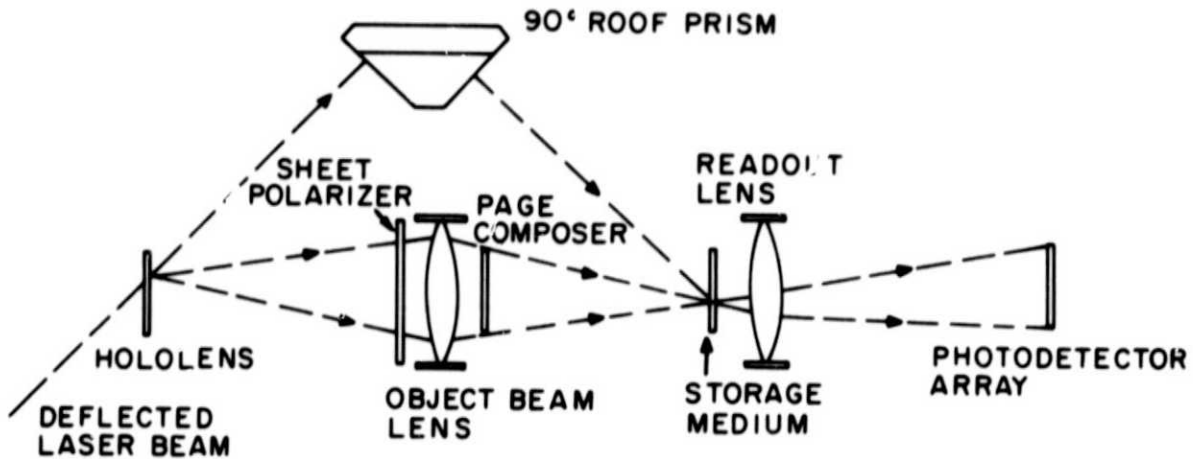


Figure 9. Schematic of a read-write holographic memory from Ref. 23.

deflection system consists of two acoustooptic deflectors at right angle with respect to each other with a resolution of 100 to 1000 positions each (total capacity of  $10^4$  to  $10^6$  bits) and with access time of 2 to 10  $\mu$ s. The hololens is a holographic optical element whose input is the light from the deflector and whose output consists of the reference beam, which is directed toward the storage medium, and a cluster of  $10^3$  to  $10^4$  low-intensity beams directed toward the page composer. This page composer (ref. 22) is an array of electronically controlled light valves that modulate the cluster of beams in a binary fashion (ON = "1", OFF = "0"). Its output and the reference beam are focussed to a 1-mm spot at the addressed location on the storage medium. With a  $10^6$  position deflector and a  $10^3$  bit page composer, the capacity of such a

page-oriented memory is  $10^9$  bits. The hologram is written-in by the application of the reference beam and the object beams from the page composer, and it is read out by the application of the reference beam alone. The output lights are converted to electrical signals by the photodetector array. In a read-write system the read-out is destructive, and the hologram must be rewritten before a new address is given to the deflectors.

#### B. Storage Medium Requirements

The storage medium is the most important component of the systems. It must have the following characteristics:

1. High Resolution Capability. - Since holographic recording involves high spatial frequencies, the resolution capability of the storage medium should be at least 1000 lines/mm.

2. Acceptable Dark Storage Time. - Present-day computer systems use a hierarchy of memories ranging from the small, fast and volatile semiconductor devices to the very large, slow and permanent tape machines. Data or programs are transferred in blocks from the slow, high-capacity units to the fast, smaller-capacity units for processing, and are later returned to the former devices. Thus, the storage ability of an active memory need not be permanent. In optical read-write memories the actual storage time would be determined by their ultimate place in the hierarchy. Depending upon usage, an acceptable storage time may range from a week to several months.

3. Acceptably Short and Equal Write and Erase Times. - The access time of core memories is of the order of  $0.4 \mu\text{s}$  and that of discs is about 3 ms. At present optical memories tend to be slower, but since the information is stored in the form of blocks or pages containing  $10^3$  to  $10^4$  bits, some speed compromise can be tolerated. An acceptable speed should be of the order of a few milliseconds per page and should be approximately the same for both writing and erasing.

4. Reversibility. - The material should be reversible in the sense that a hologram should be erasable upon illumination. This implies that the read-out with the reference beam must be destructive, just as in core memories. However, to retain the information a rewrite step must be included in the memory cycle. This situation is acceptable if the writing speed is high enough, i.e., if the storage medium is sensitive enough, so as not to increase the cycle time beyond practical limits.

5. Low Noise. - Due to the transmission losses through the optical components, the amount of light reaching the storage medium is of the order of 5% of the laser output. The storage medium may contain light-scattering structures that may broadcast light over the photodetector array and reduce the signal-to-noise ratio of the system. This "noise" introduced by the storage medium limits the system's capacity.

Although several materials have been studied as potential storage media for holographic memories, iron-doped  $\text{LiNbO}_3$  is particularly suitable because it has the above characteristics to a large extent. The major drawback is still insufficient sensitivity to make a practical memory. However, it is very promising because of its ease of preparation and because of the possibility that its sensitivity can be further improved.

#### C. Components Limitations and Projected Performance

In a typical optical memory the efficiency of the deflection system (about 20 to 25%) and the transmission and reflection losses through the various optical components are such that only about 5% of the total light reaches the storage medium. From a 1-W laser, only about 50 mW of light is available at the storage medium for writing and reading-erasing. About 10% of this amount (the hololens output) is split into the individual beams to be coded by the page composers and to be stored holographically in the storage medium. For a page composer size of  $10^3$

bits, the reference-to-object beam ratio for each bit is  $10^4$ , taking into account the effect of the hololens, and the modulation index is  $m = 0.02$ . The important question is: with only 50 mW of total light available at the storage medium, what is the write-erase cycle time that can be expected in a memory made from the improved material? Also, since the modulation index  $m$  is small, and the holographic efficiency is proportional to its square, the efficiency per bit is expected to be small. Then, with a writing time short and equal to the erase time, with the low light level and low modulation index, will we get a signal high enough at the detectors to have reasonable error rates?

To answer these questions from the available theory and verify them experimentally, let us define a suitable erase time  $T_E$  as the time required with the available light to erase a hologram to one-tenth of its initial value. From Eq. (22) the erase time thus defined is obtained by writing

$$0.1 = \exp(-2 I_0 T_E / C) = \exp(-2 T_E / T_0). \quad (23)$$

This gives

$$T_E = 1.15 T_0 = 1.15 C / I_0. \quad (24)$$

To estimate the amount of light per bit at the photodetectors we note that, if the writing time  $T_W$  is made equal to  $T_E$ , the hologram efficiency reaches about four-tenths of its saturation value in the time  $T_W$ . Due to the absorption of the heavily reduced samples and their required small thickness, the measured saturation efficiency in our samples for  $m = 1$  is of the order of 0.03. With  $m = 0.02$ , the efficiency per bit is then  $\sim 10^{-6}$ . Assuming that a total 50 mW of light is available to make the holograms and that the hologram diameter is 1 mm, we obtain  $I_0 = 64 \text{ mW/mm}^2$ . With a typical  $\text{LiNbO}_3:\text{Fe}$  sample having

$C = 1.7 \text{ mJ/mm}^2$  we obtain 30 ms for  $T_W$  and  $T_E$ , and 50 nW per bit at the photodetectors. This amount should be easily detected with a well-designed photodiode and sense amplifier system.

#### D. Memory Simulation

The setup of Fig. 10 simulates a memory with the parameters that have just been described. The hololens with 10% efficiency is represented by a 10:1 beam splitter; a  $10^3$  bit page composer is simulated by

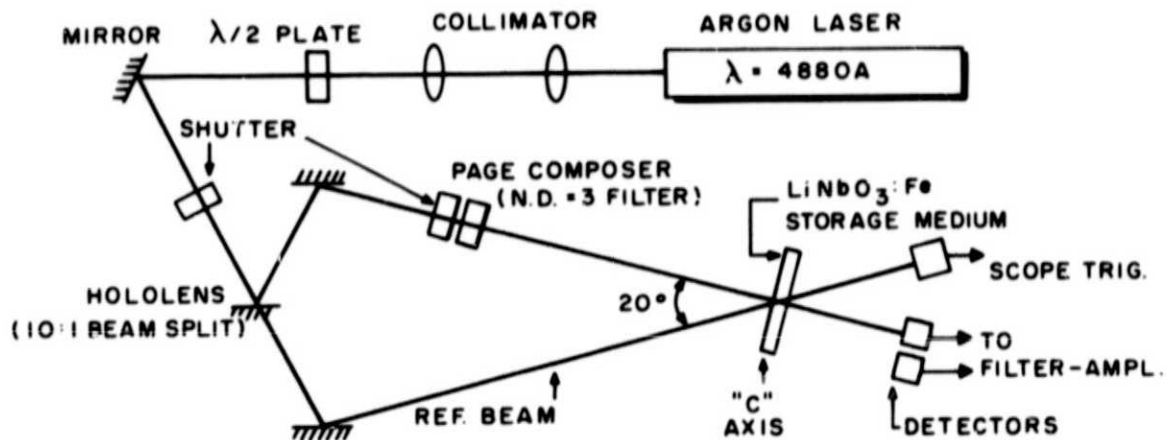
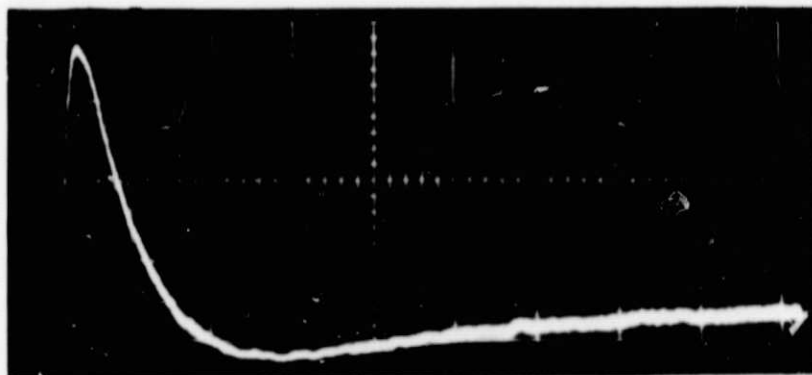


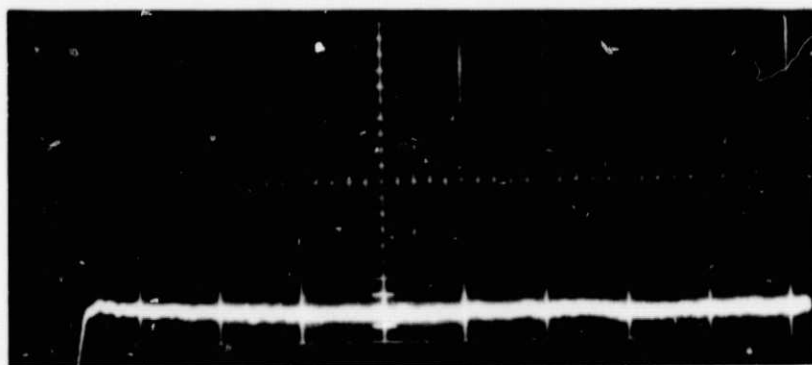
Figure 10. Simulation of the light levels in a page-oriented read-write holographic memory with  $10^3$  bits per page.

the neutral density filter having a transmission of  $10^{-3}$ . This gives the desired  $10^4$  beam ratio between the reference and object beams for each bit in a page. The light source is the 488-nm line of an argon ion laser. We adjust the laser output and use some optics to obtain a total light of 50 mW on a 1-mm-diameter spot on the storage medium. To improve the detector signal-to-noise ratio, we used differential detection with two PIN diodes and a band-limited high gain differential amplifier. The detection sensitivity of the system was about  $10^{-11}$  W.

With the setup described above, holograms were written in and read out in 30 ms each. The resulting sense signal upon read-out is shown in Fig. 11. The signal corresponds to about 9 nW of light per



(a)



(b)

Figure 11. (a) Read-out signal of simulated memory (binary "1"). Horiz. = 20 ms/div., vert. = 2.5 nW/div. (b) Read-out of a "0".

bit, or a diffraction efficiency of about  $10^{-7}$ . Although the detected light is small, the signal-to-noise ratio is very high, of the order of 27 dB, clearly demonstrating the feasibility of the system. Table III contains a complete set of experimental data for the simulated memory.

Table III. - Optical Memory Simulation Data

Wavelength	4880 Å	Reference Beam	47 mW (60 mW/mm <sup>2</sup> )
Storage Medium	Fe-LiNbO <sub>3</sub> (C=1.7mJ/mm <sup>2</sup> )	Material Relaxation Time	26 ms
Hologram Diameter	1 mm	Write or Erase Time	30 ms
Hololens Efficiency	10%	Systems Sensitivity	$1.3 \times 10^{-11}$ W
Page Composer	$10^3$ bits	Sense Signal	$9.25 \times 10^{-9}$ W
Beam Angle	20° (800 lines/mm)	SNR(with differential detection)	>27 dB

#### IV. CONCLUSIONS

Holographic memories can be viable if their speed can be made competitive with other systems of comparable capacity. The major component affecting the speed is the storage medium. Photorefractive materials are potential candidates for the role of storage media, but their sensitivity is generally low. However, the sensitivity of lithium niobate doped with iron can be controlled by heavy chemical reduction of lightly doped samples. The most practical method of chemical reduction involves annealing the crystal in the presence of a powdered salt such as lithium carbonate. This has yielded an improvement in optical sensitivity by a factor of about 38. The improvements have made it possible to evaluate the possible performance of a read-write memory using this material. Results on a simulated system indicate a cycle time of 60 ms with a high signal-to-noise ratio. Although still too slow for a practical system, this represents an improvement of two orders of magnitude over the performance of earlier experimental prototypes (ref. 5).

## REFERENCES

1. L. S. Cosentino et al., OPTICAL MEMORY DEVELOPMENT, Vol. I - Prototype Memory System, Interim Report, Contract NAS8-26808, November 1972.
2. R. A. Gange and R. S. Mezrich, OPTICAL MEMORY DEVELOPMENT, Vol. II - Gain-Assisted Holographic Storage Media, Interim Report, Contract NAS8-26808, November 1972.
3. L. S. Cosentino, E. M. Nagle, and W. C. Stewart, OPTICAL MEMORY DEVELOPMENT, Vol. III - The Membrane Light Valve Page Composer, Interim Report, Contract NAS8-26808, November 1972.
4. W. C. Stewart, R. S. Mezrich, L. S. Cosentino, E. M. Nagle, F. S. Wendt, and R. D. Lohman, "An Experimental Read-Write Holographic Memory," *RCA Review* 34, (1973).
5. W. Phillips and D. L. Staebler, "Control of the Fe<sup>2+</sup> Concentration in Iron-doped Lithium Niobate," *J. Electronic Materials* 3, 601 (1974).
6. A. Ashkin, G. D. Boyd, J. M. Dziedzic, R. G. Smith, A. A. Ballman, J. J. Levinstein, and K. Nassau, "Optically-Induced Refractive Index Inhomogeneities in LiNbO<sub>3</sub> and LiTaO<sub>3</sub>," *Appl. Phys. Letters* 9, 72 (1966).
7. F. S. Chen, "A Laser-Induced Inhomogeneity of Refractive Indices in KTN," *J. Appl. Phys.* 38, 3418 (1967).
8. D. von der Linde, A. M. Glass, and K. F. Rodgers, "Multiphoton Photorefractive Processes for Optical Storage in LiNbO<sub>3</sub>," *Appl. Phys. Letters* 25, 155 (1974); also, "High-Sensitivity Optical Recording in KTN by Two-Photon Absorption," *Appl Phys. Letters* 26, 22 (1975).
9. J. J. Amodei, "Electron Diffusion Effects During Hologram Recordings in Crystals," *Appl. Phys. Letters* 18, 22 (1971).
10. G. E. Peterson, A. M. Glass, and T. J. Negran, "Control of the Susceptibility of Lithium Niobate to Laser-Induced Refractive Index Changes," *Appl. Phys. Letters* 19, 130 (1971).
11. P. V. Lenzo, E. G. Spencer, and K. Nassau, "Electro-Optic Coefficients in Single-Domain Ferroelectric Lithium Niobate," *J. Opt. Soc. Amer.* 56, 633 (1966).
12. J. F. Nye, *Physical Properties of Crystals*, (Oxford Press, 1969) p. 252.
13. G. A. Alphonse, R. C. Alig, D. L. Staebler, and W. Phillips, "Time-Dependent Characteristics of Photo-Induced Space Charge Fields and Phase Holograms in Lithium Niobate and Other Photorefractive Media," *RCA Review* 36, 213 (1975).